hep-ph/9512441

KA-TP-16-1995

Production of neutral MSSM Higgs bosons in e^+e^- collisions: a complete 1-loop calculation.

V. Driesen, W. Hollik, J. Rosiek*
Institut für Theoretische Physik
Universität Karlsruhe, D-76128 Karlsruhe, Germany

December 1995

Abstract

We present the first complete 1-loop diagrammatic calculation of the cross sections for the neutral Higgs production processes $e^+e^- \to Z^0h^0$ and $e^+e^- \to A^0h^0$ in the minimal supersymmetric standard model. We compare the results from the diagrammatic calculation with the corresponding ones of the simpler and compact effective potential approximation and discuss the typical size of the differences.

*on leave of absence from Institute of Theoretical Physics, Warsaw University

1 Introduction

The Minimal Supersymmetric Standard Model (MSSM) predicts at least one light neutral scalar Higgs particle with mass below $\sim$ 150 GeV. In order to experimentally detect possible signals of Higgs bosons and to trace back as far as possible the physical origin of a produced scalar particle, detailed studies for the decay and production processes of Higgs boson are required.

As has been discovered several years ago [1-3], radiative corrections in the MSSM Higgs sector are large and have to be taken into account for phenomenological studies. Several methods have been developed to calculate the radiative corrections to the MSSM Higgs boson masses, production and decay rates. Three main approaches have been used for the calculation of 1-loop corrections:

a) The Effective Potential Approach (EPA) [2]: This method computes the dominant correction to the Higgs boson mass spectrum and coupling constants in a simple and fast way and is thus most suitable for numerical calculations, e.g. in Monte Carlo studies. In its practical realizations, it is based on the following approximations:

   - only the corrections to the 2-point Green's functions are included, and only the contributions from top/stop and bottom/sbottom are taken into account
   - the Green's functions are evaluated at momentum $p^2 = 0$, thus neglecting the momentum dependence.

   The EPA leads to expressions for the cross sections and decay branching ratios in an effective Born approximation, where the tree level quantities are replaced by the corrected Higgs boson masses and mixing angles.

b) The Renormalization Group approach (RGE) [3]. This method also leads to an effective Born approximation in the formulae for cross sections. The 1-loop corrected Higgs boson masses and couplings are obtained by using RG equations. Large logarithmic terms can be resummed, but realistic mass spectra are not covered by this method since it relies on an effective SUSY scale. The momentum dependence of the self-energies and 3- and 4-point functions are neglected also in this approach.

c) The diagrammatic calculation (Feynman Diagram Calculation, FDC) [4, 5]: The masses are calculated from the pole positions of the Higgs propagators, and the cross sections are obtained from the full set of 1-loop diagrams contributing to the amplitudes. The version of ref. [4] is based on the on-shell renormalization scheme. It takes into account:

– the most general form of the MSSM lagrangian with soft breaking terms,
– the virtual contributions from all the particles of the MSSM spectrum,
– all 2-, 3- and 4-point Green's functions for a given process with Higgs particles,
– the momentum dependence of the Green's functions,
– the leading reducible diagrams of higher orders corrections.

This method is technically most complicated, but also most accurate at the 1-loop level and can be used as the reference frame for simpler methods. Moreover, it allows to study the full parameter dependence of cross sections and decay rates.

The experimental searches for Higgs bosons at LEP1 [6] and studies for the future searches at higher energies [7] conventionally make use of the most compact effective potential approximation. The phenomenological study in ref. [8] for LEP2 and higher energies, was done in the FDC, but still not complete at 1-loop order. A check of the quality of the simpler approximations and estimates of their reliability in various energy and parameter ranges have also not yet been performed so far.

In this paper we present the first complete 1-loop diagrammatic results for the cross sections for the neutral Higgs production processes $e^+e^- \to Z^0h^0$ and $e^+e^- \to A^0h^0$. In addition, we compare the results from the complete diagrammatic calculation with the corresponding ones of the simpler and compact effective potential approximation and discuss the typical size of the differences.

Recently some papers on the leading 2-loop corrections to the CP-even MSSM Higgs boson masses have been published [9]. The main conclusion is that 2-loop corrections are also significant and tend to compensate partially the effects of 1-loop corrections. The calculations are based on the EPA and RG methods. Since one of the main emphasis of our study is to figure out the difference between complete and approximate results in a given order, we have not implemented the 2-loop terms. They would improve the 1-loop FDC results in the same way as the approximations and thus do not influence the remaining differences which can only be obtained by an explicit diagrammatic calculation.

In Section 2 we give a short description of the computational schemes for the masses and cross sections. This is followed in Section 3 by a discussion of the numerical results and a comparison of the various approximations.

2 Outline of the calculations

The tree level potential for the neutral MSSM Higgs bosons can be written as:

$$V^{(0)} = m_1^2 H_1^2 + m_2^2 H_2^2 + \epsilon_{ij}(m_{12}^2 H_1^i H_2^j + H.c.) + \frac{1}{8}(g^2 + g'^2)(H_1^2 - H_2^2)^2 + \frac{1}{4}g^2(H_1 H_2)^2 \quad (1)$$

Diagonalization of the mass matrices for the CP-even and the CP-odd scalars, following from the potential (1), leads to three physical particles: two CP-even Higgs bosons H^0,h^0 and one CP-odd Higgs boson A^0 , and defines their tree-level masses m_H , m_h and m_A , with $m_H > m_h$, and the mixing angles α, β.

The 1-loop radiative corrections significantly modify the tree level relations between the masses and mixing angles. The way of calculating the radiative corrections in the EPA and FDC methods is briefly described as follows:

In the EPA, the tree level potential $V^{(0)}$ is improved by adding the 1-loop terms [2]:

$$V^{(1)}(Q^2) = V^{(0)}(Q^2) + \Delta V^{(1)}(Q^2) \tag{2}$$

where

$$\Delta V^{(1)}(Q^2) = \frac{1}{64\pi^2} \sum_{\substack{quarks \\ squarks}} \mathrm{Str}\mathcal{M}^4 \left(\log \frac{\mathcal{M}^2}{Q^2} - \frac{3}{2} \right) \tag{3}$$

$V^{(0)}(Q^2)$ is the tree level potential evaluated with couplings renormalized at the scale Q^2, and Str denotes the supertrace over the third generation of quark and squark fields contributing to the generalized squared mass matrix $\mathcal{M}^2$.

The full 1-loop potential $V^{(1)}$ is rediagonalized yielding the 1-loop corrected physical masses M_H , M_h and the effective mixing angle α_{eff} . Thereby M_A and $\tan\beta$ are usually considered as the free input parameters. Explicit formulae for the 1-loop corrected CP-even Higgs mass matrices can be found in first paper of ref. [2]. The physical Higgs boson masses and 1-loop mixing angles are used in the Born formulae for the production cross sections and decay rates.

In many experimental neutral MSSM Higgs searches a simplified version of the EPA ("ϵ-approximation") was used in the analysis of the experimental data. In this approximation only the leading correction coming from the top and stop quark loops to the Higgs mass matrix is included. In addition, the effects of the sfermion mixing are neglected. In this case the corrected Higgs mass matrix has the simple form:

$$\mathcal{M}_{CP-even} = \frac{\sin 2\beta}{2} \begin{pmatrix} \cot\beta M_Z^2 + \tan\beta M_A^2 & -M_Z^2 - M_A^2 \\ -M_Z^2 - M_A^2 & \tan\beta M_Z^2 + \cot\beta M_A^2 + \epsilon \end{pmatrix} \tag{4}$$

where ϵ summarizes the leading 1-loop corrections:

$$\epsilon = \frac{3 G_F m_t^4}{\sqrt{2}\pi^2 \sin^2\beta} \log\left(\frac{M_{\tilde{t}_1} M_{\tilde{t}_2}}{m_t^2} \right). \tag{5}$$

This yields:

$$M_{H,h}^2 = \frac{M_A^2 + M_Z^2 + \epsilon}{2} \pm \sqrt{\frac{(M_A^2 + M_Z^2)^2 + \epsilon^2}{4} - M_A^2 M_Z^2 \cos^2 2\beta + \frac{\epsilon \cos 2\beta}{2}(M_A^2 - M_Z^2)} \tag{6}$$

$$\tan\alpha_{eff} = \frac{-(M_A^2 + M_Z^2)\tan\beta}{M_Z^2 + M_A^2\tan^2\beta - (1+\tan^2\beta)M_h^2} \tag{7}$$

The 1-loop corrected Higgs boson masses M_H , M_h and the effective mixing angle α_{eff} thus depend on only one extra SUSY parameter, namely the product $M_{\tilde{t}_1}M_{\tilde{t}_2}$ of the scalar top mass eigenvalues, in addition to the tree level parameters M_A and $\tan\beta$.

In the FDC approach the 1-loop physical Higgs boson masses are obtained as the pole positions of the dressed scalar propagators. In order to obtain accurate values of the masses, also the leading reducible terms of higher order have to be taken into account. M_H^2 and M_h^2 are given by the solution of the equation of the form:

$$\mathrm{Re}\left[\left(p^2 - m_h^2 - \Sigma_{hh}(p^2)\right)\left(p^2 - m_H^2 - \Sigma_{HH}(p^2)\right) - \Sigma_{hH}^2(p^2)\right] = 0 \tag{8}$$

For the calculations of the cross sections we need the full set of scalar 2-point functions, and also the 3- and 4-point Green's functions are taken into account. In Figure 1 the diagrams contributing to the $e^+e^- \to Z^0h^0, A^0h^0$ process are collected. Specially important is the diagram f) in Figure 1, illustrating the h^0 -H^0 mixing on the external scalar line, as this mixing corresponds in a good approximation to the effect of introducing the effective mixing angle α_{eff} into the Born formulae. The formulae for the cross sections obtained in the FDC now differ from the Born expressions, because not only the effective values of the masses are corrected but also new form factors and momentum dependent effects are considered. The analytic formulae for the cross sections for the processes $e^+e^- \to Z^0h^0, A^0h^0$, including all but the box and 1-loop $e^+e^-h^0$ vertex contributions, can be found in the first paper of ref. [4]. Effects of box contributions are discussed in the third paper of ref. [4]. In the present paper we include also the 1-loop contributions to the $e^+e^-h^0$ vertex in the cross section calculation. Note that the diagrams h), i), j) of Figure 1 are not part of the phenomenological study in [8].

3 Results on Higgs masses and production cross sections

In this section we present the results for Z^0h^0 and A^0h^0 production from the complete diagrammatic 1-loop calculation (FDC) and discuss the quality of simpler approximations:

- the effective potential approach (EPA), as described above,
- the simplified EPA with sfermion mixing and bottom/sbottom loop neglected ("ϵ-approximation"), based on eqs. (4-7).

In order to give an orientation about the accuracy of the approximations we show comparisons of the various methods in the different regions of the parameter space.

From the theoretical point of view, the most convenient parameters for the Higgs sector are the mass M_A of the CP-odd Higgs boson and the ratio $\tan\beta = \frac{v_2}{v_1}$. From the experimental point of view it is more natural to use the mass M_h of the lighter CP-even Higgs instead of the formal quantity $\tan\beta$. This, however, is technically more complicated for the calculational scheme. In the first part of this discussion we follow the conventional way of presentation and choose $\tan\beta$ as a free input parameter. In the second part we replace $\tan\beta$ in favor of the physical neutral Higgs mass M_h . This has the advantage to directly get the theoretical results for the production cross sections for the case that a Higgs boson is found and its mass has been determined.

As a first step, we put together the predictions of the various methods for the physical h^0 mass M_h for given M_A and $\tan\beta$. Figure 2 is based on the parameters listed in Table 1. μ is the parameter describing the Higgs doublet mixing in the MSSM superpotential. M_2

Parameter	m_t	M_A	M_{sq}	M_{sl}	M_2	μ	$A_t = A_b$
Value (GeV)	175	70	1000	300	1000	500	1000

Table 1: Parameters used for the numerical analysis.

denotes the SU(2) gaugino mass parameter. For the U(1) gaugino mass we use the value $M_1 = \frac{5}{3}\tan^2\theta_W M_2$, suggested by GUT constraints. μ, M_2 determine the chargino and neutralino sectors (for the detailed expressions see for example [10]). M_{sq}, M_{sl}, A_t and A_b are the parameters entering the sfermion mass matrices. For simplicity we assume a common value M_{sq} for all generations of squarks, and a common M_{sl} for sleptons. For the scalar top mass matrix one has[1]:

$$\mathcal{M}_{stop} = \begin{pmatrix} (\frac{1}{2} - \frac{2}{3}\sin^2\theta_W)M_Z^2\cos 2\beta + m_t^2 + M_{sq}^2 & -m_t(\mu\cot\beta + A_t) \\ -m_t(\mu\cot\beta + A_t) & \frac{2}{3}\sin^2\theta_W M_Z^2 \cos 2\beta + m_t^2 + M_{sq}^2 \end{pmatrix} \quad (9)$$

In Figure 3, only the mixing parameters have been turned off, i.e. $A_t, A_b, \mu \approx 0$ in order to have a situation where the "ϵ-approximation" should be most suitable. Indeed, the "ϵ-approximation" and the full EPA are almost identical in this case.

[1] Actually in the calculation we use 6×6 sfermion mass matrices, including the possibility of intergenerational mixing [10]. Effects of this mixing appear for example when the mass parameters for different sfermion generations are not equal to each other.

We define the relative differences for the masses with respect to the FDC as follows:

$$\delta M_h^{EPA,\epsilon} = \frac{M_h^{FDC} - M_h^{EPA,\epsilon}}{M_h^{FDC}}. \tag{10}$$

As shown in Figure 2, the values for M_h obtained by FDC and EPA are rather close and differ by less than 4%. FDC gives lower values of M_h than the approximations. This is a general result, valid for all the parameter choices, and connected with the negative contribution to M_h from the gaugino/higgsino sector which is not included in the EPA calculations. Figure 2 also shows that the "ϵ-approximation" for M_h differs more significantly from the FDC result. The reason is just the neglected mixing term.

The results for the heavier CP-even scalar mass M_H from FDC and EPA are again in good agreement. The "ϵ-approximation" for this case yields masses typically 15%-20% different from the FDC values.

Figures 4, 5 display comparisons of the cross sections for the processes $e^+e^- \to Z^0h^0, A^0h^0$ for two center-of-mass energies: 205 GeV (Figure 4) and 500 GeV (Figure 5). The parameters are the same as the ones listed in Table 1. In analogy to (10) we define:

$$\delta\sigma_{Zh}^{EPA,\epsilon} = \frac{\sigma_{Zh}^{FDC} - \sigma_{Zh}^{EPA,\epsilon}}{\sigma_{Zh}^{FDC}} \qquad \sigma_{Zh} = \sigma(e^+e^- \to Z^0h^0)$$

$$\delta\sigma_{Ah}^{EPA,\epsilon} = \frac{\sigma_{Ah}^{FDC} - \sigma_{Ah}^{EPA,\epsilon}}{\sigma_{Ah}^{FDC}} \qquad \sigma_{Ah} = \sigma(e^+e^- \to h^0A^0). \tag{11}$$

As one can see from both figures, the EPA predictions follow in general more closely the FDC results than the "ϵ-approximation" . The numerical differences can reach 10-20% at 205 GeV and 30% at 500 GeV. They become more important with increasing energies, exceeding 40% at 1 TeV. Note, however, that in the region of large cross sections the EPA accuracy is better (20% up to 500 GeV).

The formally large relative deviations appearing in σ_{Zh} for large $\tan\beta$ are not important from a practical point of view since the cross section is extremely small in this region.

The less accurate number obtained in the "ϵ-approximation" can again be addressed to the neglected mixing effects in the scalar quark sector.

To give a more global impression of the typical size of the differences between the EPA and FDC results, we have chosen 1000 random points (for each $\sqrt{s}$ value in Table 2) from the hypercube in the MSSM parameters space with the following bounds:

$0.5 < \tan\beta < 50$	5 GeV $< M_A <$ 150 GeV
-500 GeV $< \mu <$ 500 GeV	200 GeV $< M_2 <$ 1000 GeV
200 GeV $< M_{sq} <$ 1000 GeV	100 GeV $< M_{sl} <$ 300 GeV
$-M_{sq} < A_t = A_b < M_{sq}$	

We calculated the quantities $|\delta M_h^{EPA}|$, $|\delta M_H^{EPA}|$, $|\delta\sigma_{Zh}^{EPA}|$ and $|\delta\sigma_{Ah}^{EPA}|$ and averaged them arithmetically over all generated points of the parameter space. The results are summarized in Table 2. It shows that the predictions of both methods deviate in particular for σ_{Zh}.

Quantity	$\sqrt{s}$ =205 GeV	$\sqrt{s}$ =500 GeV	$\sqrt{s}$ =1 TeV
$\lvert\delta M_h^{EPA}\rvert$	2.7%	2.7%	2.7%
$\lvert\delta M_H^{EPA}\rvert$	2.2%	2.2%	2.2%
$\lvert\delta\sigma_{Zh}^{EPA}\rvert$	22%	29%	32%
$\lvert\delta\sigma_{Ah}^{EPA}\rvert$	5.5%	9.5%	15%

Table 2: Differences between the EPA and FDC predictions averaged over a random sample of parameters.

We have analyzed also the dependence of the differences between the EPA and the FDC predictions on the SUSY parameters: sfermion and gaugino masses, μ parameter and sfermion mixing parameters. In most cases the variation of those parameters does not have a large effect on the size of the differences between the EPA and FDC. The only exception is the gaugino mass, which is completely absent in the EPA. For a relatively heavy A^0 ($M_A > 50$ GeV) the increase of M_2 causes a slow change of δM_h^{EPA} , $\delta\sigma_{Zh}^{EPA}$, $\delta\sigma_{Ah}^{EPA}$ (see Figure 6). This effect can be quite dramatic for small $M_A \sim 5-20$ GeV and M_2 around 1 TeV, but such low M_A values are however already excluded by the LEP1 measurements.

We now turn to the more physical parametrization of the cross sections in terms of the two Higgs boson masses M_A and M_h . This parameterization is more clumsy in the calculations, but it has the advantage of physically well defined input quantities avoiding possible confusions from different renormalization schemes. Technically, $\tan\beta$ is calculated for given M_h , M_A and the other input parameters. Varying M_h (M_A and other input quantities fixed) we thus obtain $\tan\beta$ and σ_{Zh}, σ_{Ah} as functions of M_h . The predictions for the cross sections are, however, in general not unique because there can be two solutions for $\tan\beta$, thus yielding two branches for fixed values of M_A .

The solutions for $\tan\beta$ are shown in Figure 7 for the input parameters of Table 1, again for the FDC and the simpler approximations. As can be seen from the figure, the differences between the $\tan\beta$ values obtained in the EPA and FDC can reach 20%. Also significant differences can occur for the cross sections, as displayed in Figure 8 where the predictions of EPA and FDC for the σ_{Zh} and σ_{Ah} are plotted as functions of M_h . The typical size of differences between the methods is 10-20% for $\sqrt{s}$ =205 GeV.

4 Summary

We presented the results from a complete 1-loop diagrammatic calculation in the MSSM for the cross sections for neutral Higgs production via $e^+e^- \to Z^0h^0$ and $e^+e^- \to A^0h^0$, including box diagrams and h^0 e^+e^- vertex contributions which were not part of previous studies for Higgs searches in the literature. Comparisons between the FDC predictions with the simpler EPA approximation have shown that the EPA has an accuracy of typically 10-20% in the parameter regions where the cross sections are large. The differences become bigger with increasing energy. They may be specially important for future high energy e^+e^- colliders. The use of the physical input variables M_A, M_h avoids ambiguities from the definition of $\tan\beta$ in higher order, but the observed differences remain of the same size. For a better accuracy, the full FDC would be required. It will also be necessary to incorporate the leading 2nd order terms since they are at least as big as the non-leading 1-loop contributions.

The library of FORTRAN codes for the calculation of the 1-loop radiative corrections in the on-shell renormalization scheme to the MSSM neutral Higgs production and decay rates [4] can be found at the URL address
http://itpaxp1.physik.uni-karlsruhe.de/~rosiek/neutral_higgs.html

Acknowledgments

This work was supported in part by the Alexander von Humboldt Stiftung, by the European Union under contract CHRX-CT92-0004 and by the Polish Committee for Scientific Research.

References

[1] S. P. Li and M. Sher, *Phys. Lett.* **B140** (1984), 339;
J. F. Gunion and A. Turski, *Phys. Rev.* **D39** (1989) 2701; **D40** (1989) 2325, 2333;
M. Berger, *Phys. Rev.* **D41** (1990) 225.

[2] J. Ellis, G. Ridolfi and F. Zwirner, *Phys. Lett.* **262B** (1991) 477;
R. Barbieri and M. Frigeni, *Phys. Lett.* **258B** (1991) 395;
A. Brignole, J. Ellis, G. Ridolfi and F. Zwirner *Phys. Lett.* **271B** (1991) 123.

[3] M. Carena, K. Sasaki and C.E.M. Wagner, *Nucl. Phys.* **381B** (1992) 66;
H.E. Haber, R. Hempfling, *Phys. Rev.* **D48** (1993) 4280:
P.H. Chankowski, S. Pokorski and J. Rosiek, *Phys. Lett.* **281B** (1992) 100.

[4] P. Chankowski, S. Pokorski, J. Rosiek *Nucl. Phys.* **B423** (1994) 437; **B423** (1994) 497;
V. Driesen, W. Hollik, *Z. Phys.* **C68** (1995) 485.

[5] A. Brignole, *Phys. Lett.* **281B** (1992) 284.

[6] ALEPH Collaboration, D. Buskulic *et al.*, *Phys. Lett.* **313B** (1993), 312;
DELPHI Collaboration, P. Abreu *et al.*, *Nucl. Phys.* **373B** (1992), 3;
L3 Collaboration, O. Adriani *et al.*, *Z. Phys.* **57C** (1993), 355;
OPAL Collaboration, R. Akers *et al.*, Preprint CERN, PPE/94-104 (1994);
J. F. Grivaz, plenary talk at International Europhysics Conference on High Energies, Brussels, July 27 - August 2, 1995; preprint LAL-95-83 (to appear in the Proceedings).

[7] *Higgs Physics*, M. Carena and P. Zerwas et al., to appear in the Proceedings of LEP2 Workshop, CERN Yellow Report, eds. G. Altarelli et al.;
Higgs Particles, in: e^+e^- Collisions at 500 GeV, DESY 92-123A,B; DESY 93-123C, ed. P. Zerwas.

[8] J. Rosiek, A. Sopczak, *Phys. Lett.* **B341** (1994) 419.

[9] R. Hempfling, A. Hoang, *Phys. Lett.* **B331** (1994) 99;
M. Carena, J.R. Espinosa, M. Quiros, C.E.M. Wagner, *Phys. Lett.* **B355** (1995) 209;
M. Carena, M. Quiros, C.E.M. Wagner, preprint CERN-TH-95-157, hep-ph/9508343.

[10] J. Rosiek, *Phys. Rev.* **D41** (1990) 3464.

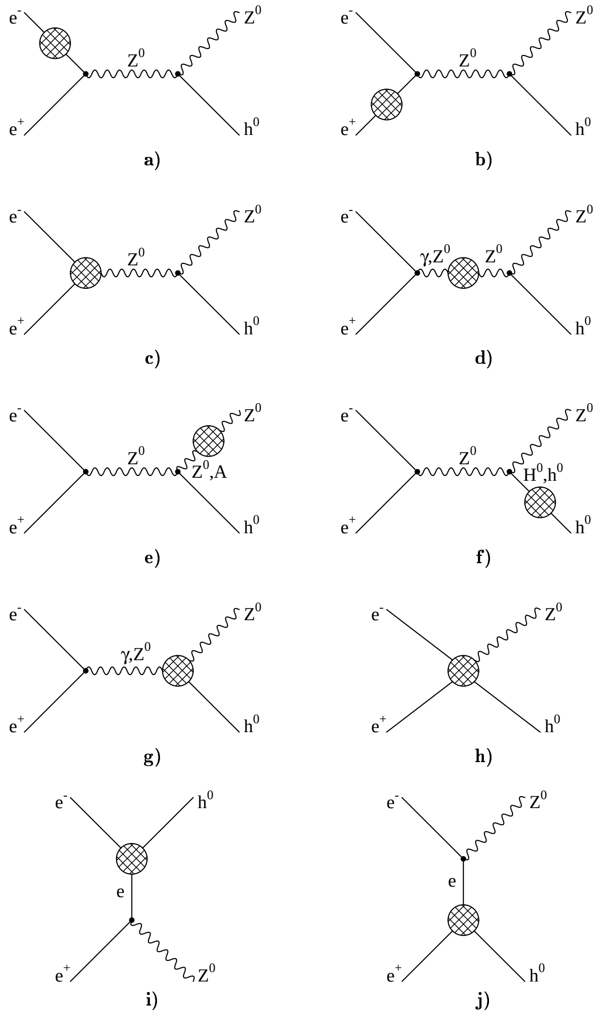

Figure 1: Classes of Feynman diagrams contributing to the $e^+e^- \to Z^0h^0$ process in the FDC approach. The diagrams contributing to the $e^+e^- \to A^0h^0$ process can be obtained by changing Z^0 into A^0 on the external line and skipping the diagrams i), j).

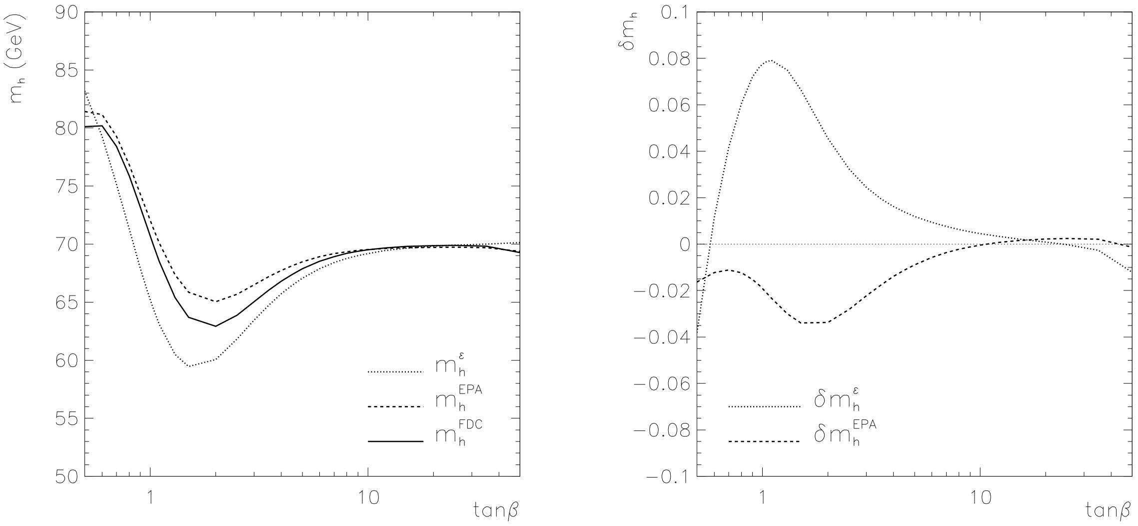

Figure 2: Comparison of the physical h^0 masses obtained in the "ϵ-approximation" , EPA and FDC. Parameters as given in Table 1.

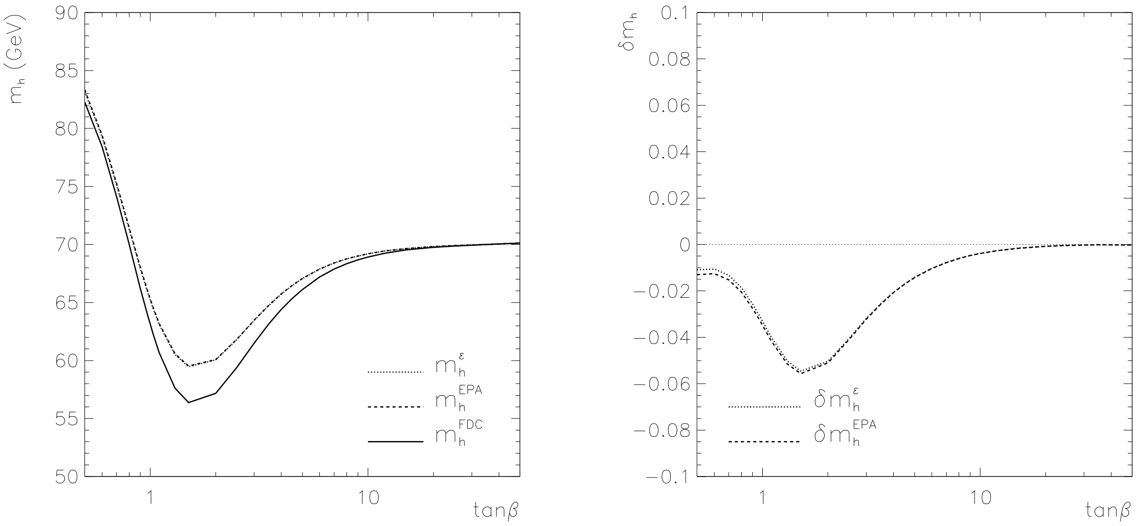

Figure 3: Comparison of the physical h^0 masses obtained in the "ϵ-approximation" , EPA and FDC. Mass parameters as given in Table 1, but mixing parameters $\mu, A_t, A_b \approx 0$.

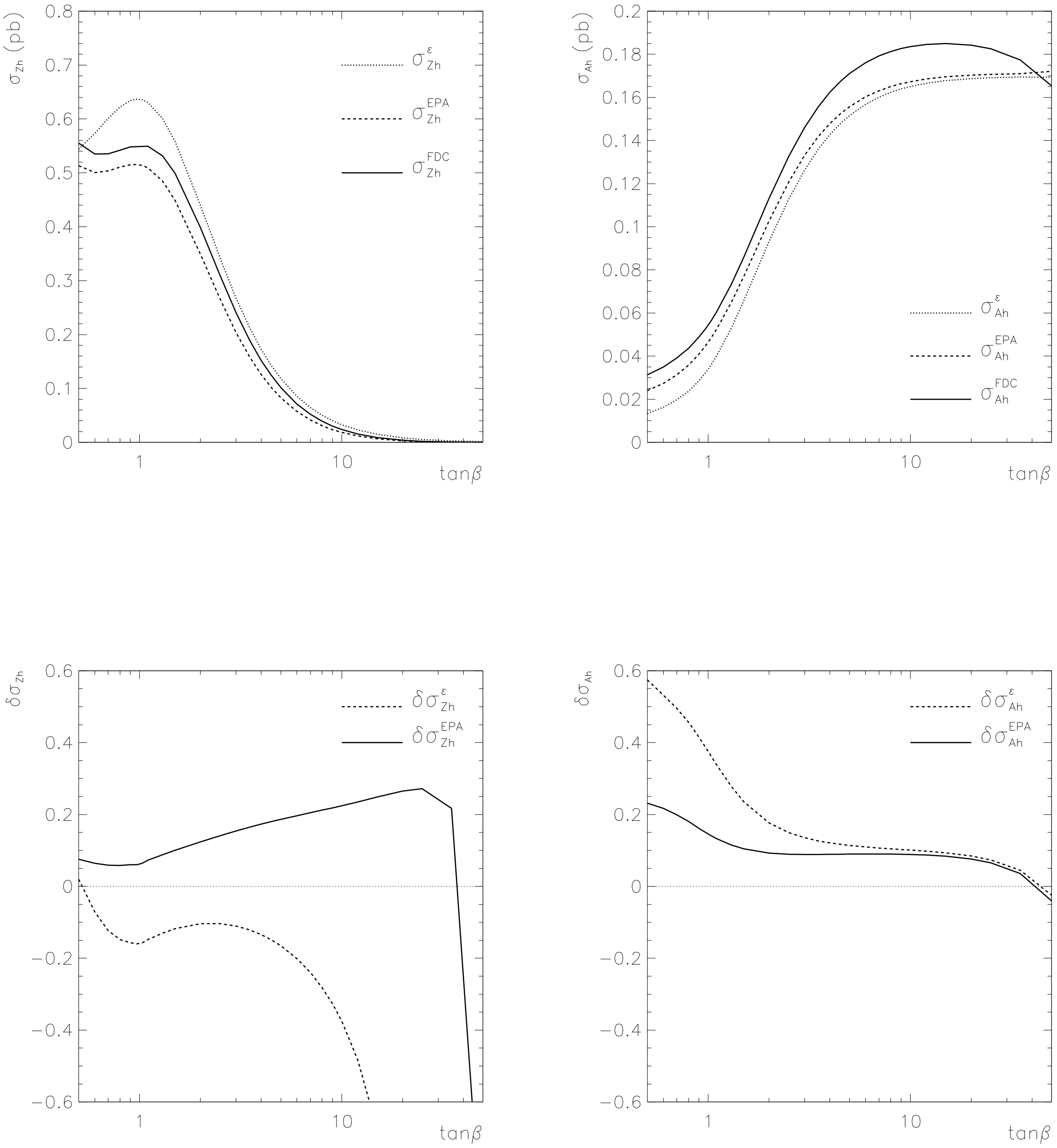

Figure 4: Comparison of the cross sections $\sigma(e^+e^- \to Z^0h^0, h^0A^0)$ obtained in the "ϵ-approximation" , EPA and FDC. Parameters as given in Table 1, center-of-mass energy $\sqrt{s} = 205$ GeV.

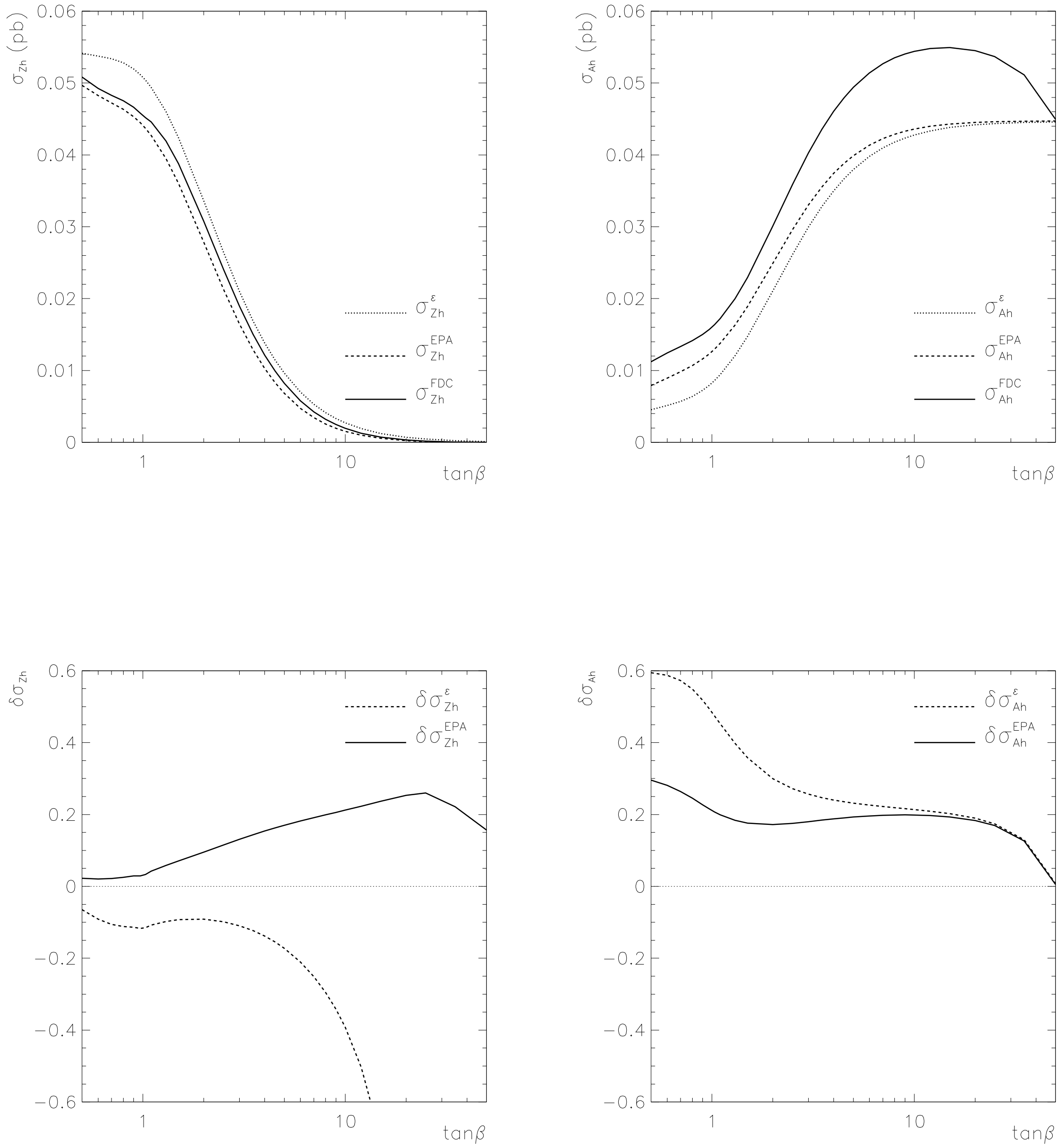

Figure 5: Comparison of the cross sections $\sigma(e^+e^- \to Z^0h^0, h^0A^0)$ obtained in the "ϵ-approximation" , EPA and FDC. Parameters defined as in Table 1, center-of-mass energy $\sqrt{s} = 500$ GeV.

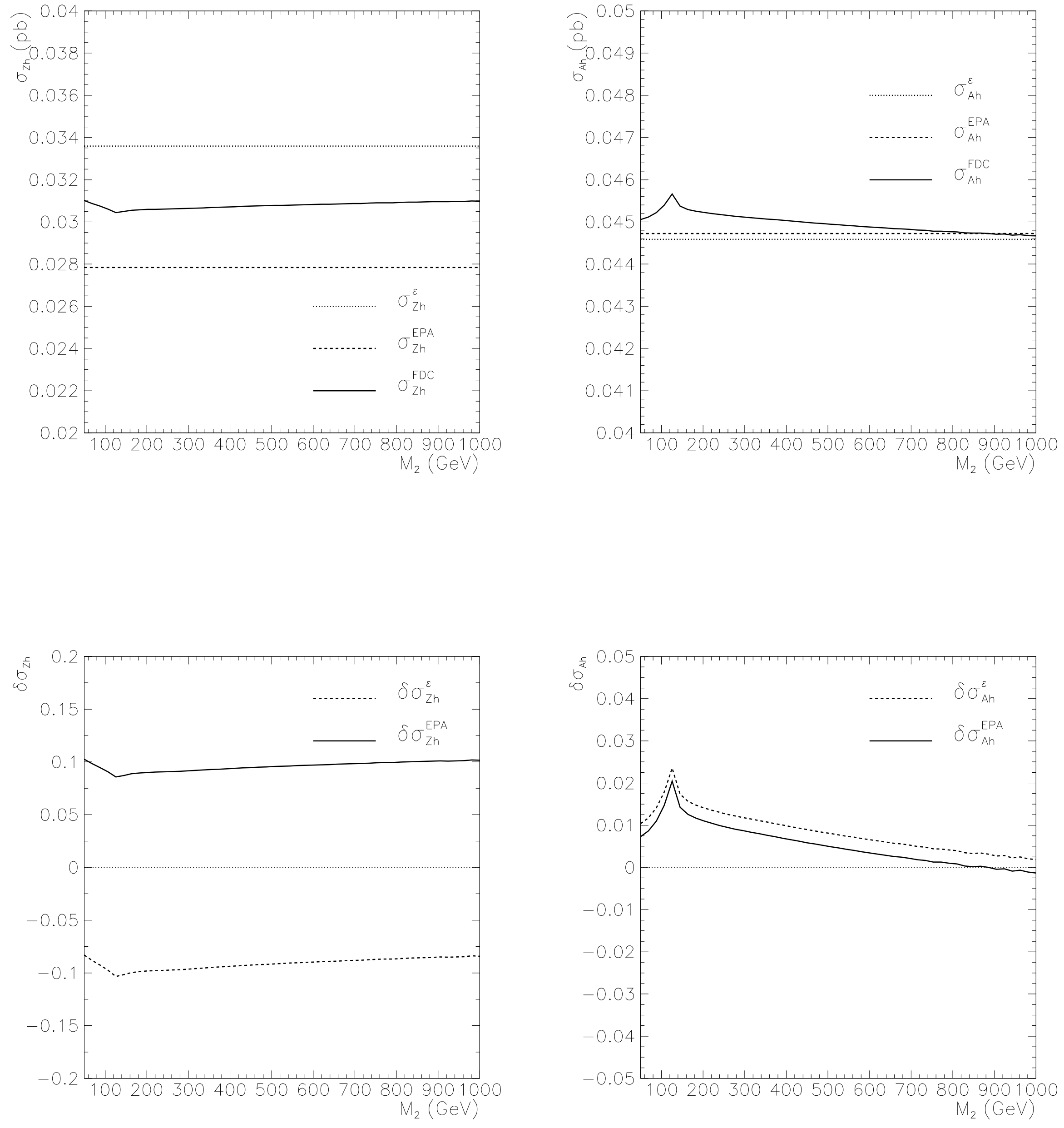

Figure 6: Comparison of the cross sections $\sigma(e^+e^- \to Z^0h^0, h^0A^0)$ as a function of M_2 in the "ϵ-approximation" , EPA and FDC. Parameters as given in Table 1. $\tan\beta = 2$ in the left plots and $\tan\beta = 50$ in the right plots. Center-of-mass energy $\sqrt{s} = 500$ GeV.

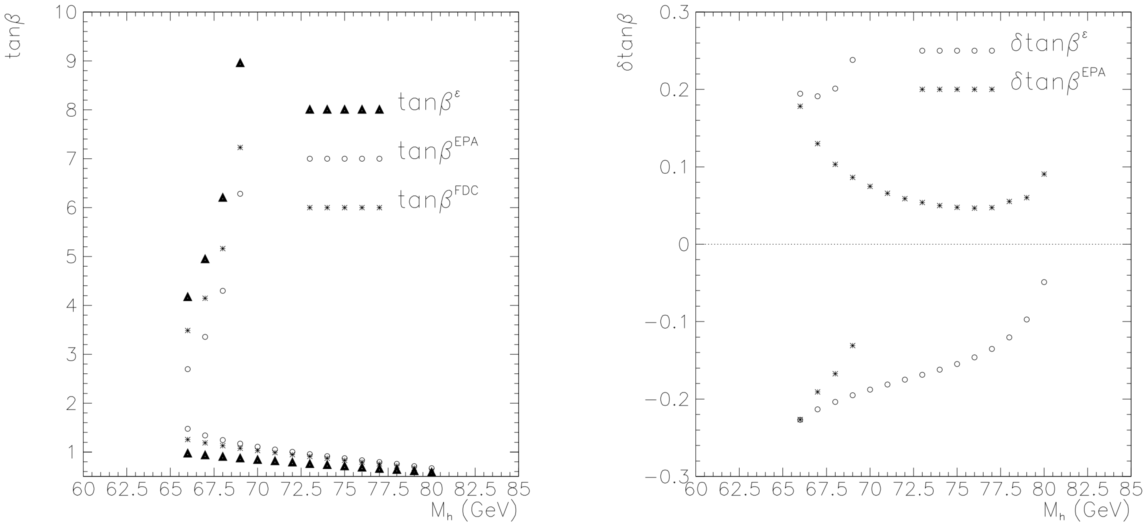

Figure 7: Comparison of the $\tan\beta$ dependence on M_h in the "ϵ-approximation" , EPA and FDC. Parameters as given in Table 1. $\delta\tan\beta$ is the relative difference from the FDC values.

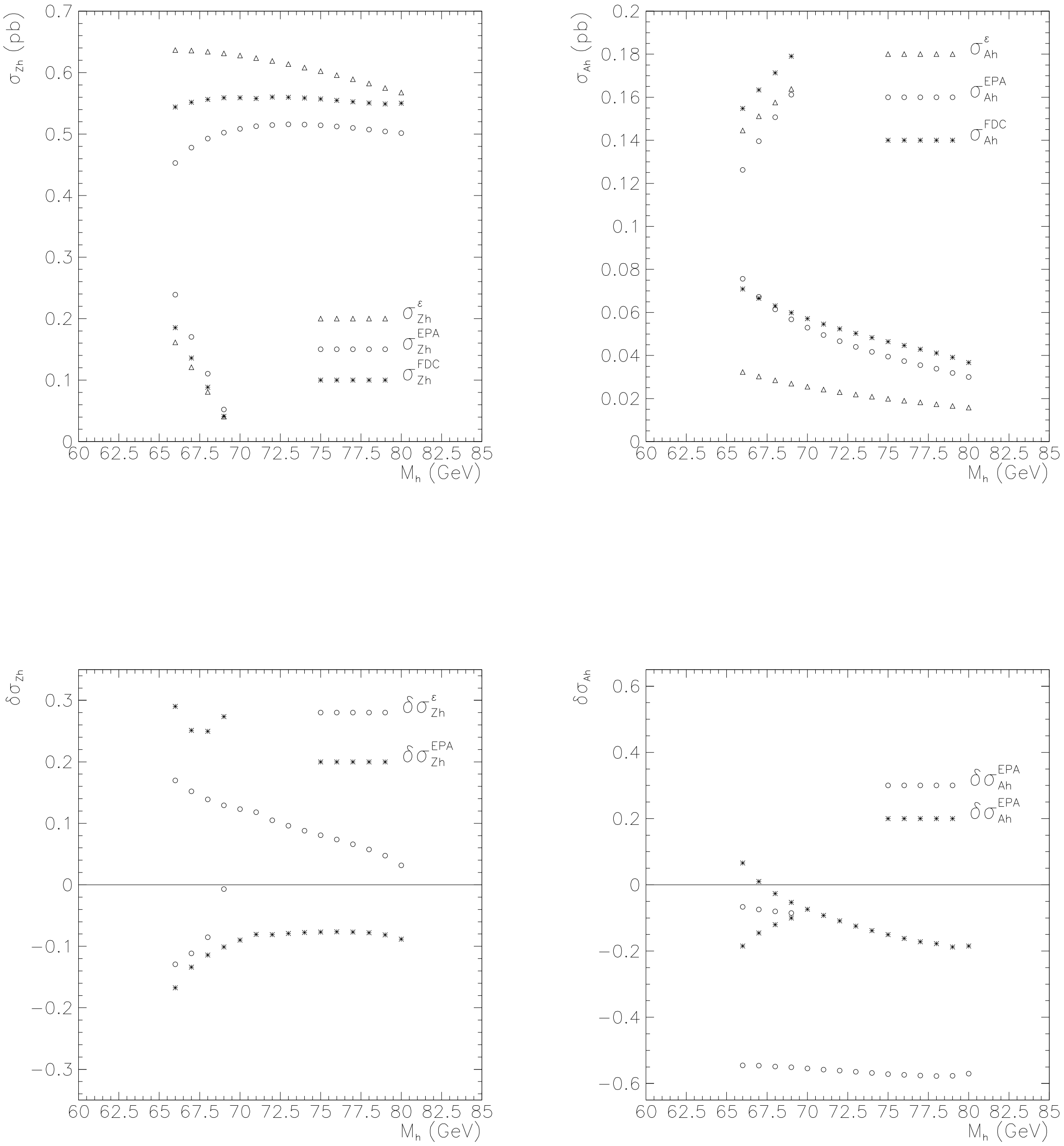

Figure 8: Comparison of the cross sections $\sigma(e^+e^- \to Z^0h^0, h^0A^0)$ as a function of M_h in the "ϵ-approximation" , EPA and FDC. Parameters as given in Table 1, center-of-mass energy $\sqrt{s} = 205$ GeV.